A 3D diamond detector for particle tracking

M. Artuso, F. Bachmair, L. Bäni, M. Bartosik, J. Beacham, V. Bellini, V. Belyaev, B. Bentele, E. Berdermann, P. Bergonzo, et al.

HAL Id: in2p3-01322643
https://hal.in2p3.fr/in2p3-01322643

Submitted on 6 Apr 2020

A 3D diamond detector for particle tracking

M. Artuso [v], F. Bachmair [z], L. Bäni [z], M. Bartosik [c], J. Beacham [o], V. Bellini [b], V. Belyaev [n], B. Bentele [u], E. Berdermann [g], P. Bergonzo [m], A. Bes [ad], J-M. Brom [i], M. Bruzzi [e], M. Cerv [c], C. Chau [r], G. Chiodini [ac], D. Chren [t], V. Cindro [k], G. Claus [i], J. Collot [ad], S. Costa [b], J. Cumalat [u], A. Dabrowski [c], R. D'Alessandro [e], W. de Boer [l], B. Dehning [c], D. Dobos [c], M. Dünser [z], V. Eremin [h], R. Eusebi [aa], G. Forcolin [x], J. Forneris [q], H. Frais-Kölbl [d], K.K. Gan [o], M. Gastal [c], M. Goffe [i], J. Goldstein [s], A. Golubev [j], L. Gonella [a], A. Gorišek [k], L. Graber [y,n], E. Grigoriev [j], J. Grosse-Knetter [y], B. Gui [o], M. Guthoff [c], I. Haughton [x], D. Hidas [p], D. Hits [z], M. Hoeferkamp [w], T. Hofmann [c], J. Hosslet [i], J-Y. Hostachy [ad], F. Hügging [a], H. Jansen [c], J. Janssen [a], H. Kagan [o], K. Kanxheri [ae], G. Kasieczka [z], R. Kass [o], F. Kassel [l], M. Kis [g], G. Kramberger [k], S. Kuleshov [j], A. Lacoste [ad], S. Lagomarsino [e], A. Lo Giudice [q], C. Maazouzi [i], I. Mandic [k], C. Mathieu [i], N. McFadden [w], G. McGoldrick [r], M. Menichelli [ae], M. Mikuž [k], A. Morozzi [ae], J. Moss [o], R. Mountain [v], S. Murphy [x], A. Oh [x], P. Olivero [q], G. Parrini [e], D. Passeri [ae], M. Pauluzzi [ae], H. Pernegger [c], R. Perrino [ac], F. Picollo [q], M. Pomorski [m], R. Potenza [b], A. Quadt [y], A. Re [q], G. Riley [ab], S. Roe [c], M. Sapinski [c], M. Scaringella [e], S. Schnetzer [p], T. Schreiner [d], S. ciortino [e], A. Scorzoni [ae], S. Seidel [w], L. Servoli [ae], A. Sfyrla [c], G. Shimchuk [j], D.S. Smith [o], B. Sopko [t], V. Sopko [t], S. Spagnolo [ac], S. Spanier [ab], K. Stenson [u], R. Stone [p], C. Sutera [b], A. Taylor [w], M. Traeger [g], D. Tromson [m], W. Trischuk [r], C. Tuve [b], L. Uplegger [f], J. Velthuis [s], N. Venturi [r], E. Vittone [q], S. Wagner [u], R. Wallny [z], J.C. Wang [v], P. Weilhammer [c], J. Weingarten [y], C. Weiss [c], T. Wengler [c], N. Wermes [a], M. Yamouni [ad], M. Zavrtanik [k]

[a] Universität Bonn, Bonn, Germany
[b] INFN/University of Catania, Catania, Italy
[c] CERN, Geneva, Switzerland
[d] FWT, Wiener Neustadt, Austria
[e] INFN/University of Florence, Florence, Italy
[f] FNAL, Batavia, USA
[g] GSI, Darmstadt, Germany
[h] Ioffe Institute, St. Petersburg, Russia
[i] IPHC, Strasbourg, France
[j] ITEP, Moscow, Russia
[k] Jožef Stefan Institute, Ljubljana, Slovenia
[l] Universität Karlsruhe, Karlsruhe, Germany
[m] CEA-LIST Technologies Avancees, Saclay, France
[n] MEPHI Institute, Moscow, Russia
[o] The Ohio State University, Columbus, OH, USA
[p] Rutgers University, Piscataway, NJ, USA
[q] University of Torino, Torino, Italy
[r] University of Toronto, Toronto, ON, Canada
[s] University of Bristol, Bristol, UK
[t] Czech Technical University, Prague, Czech Republic
[u] University of Colorado, Boulder, CO, USA
[v] Syracuse University, Syracuse, NY, USA
[w] University of New Mexico, Albuquerque, NM, USA
[x] University of Manchester, Manchester, UK
[y] Universität Göttingen, Göttingen, Germany
[z] ETH Zürich, Zürich, Switzerland
[aa] Texas A& M, College Park Station, TX, USA
[ab] University of Tennessee, Knoxville, TN, USA
[ac] INFN-Lecce, Lecce, Italy
[ad] LPSC-Grenoble, Grenoble, France
[ae] INFN-Perugia, Perugia, Italy

Corresponding author. *E-mail address:* lgraber@uni-goettingen.de (L. Graber).

Abstract

In the present study, results towards the development of a 3D diamond sensor are presented. Conductive channels are produced inside the sensor bulk using a femtosecond laser. This electrode geometry allows full charge collection even for low quality diamond sensors. Results from testbeam show that charge is collected by these electrodes. In order to understand the channel growth parameters, with the goal of producing low resistivity channels, the conductive channels produced with a different laser setup are evaluated by Raman spectroscopy.

1.   Introduction

Diamond sensors are radiation tolerant enough to be used in the innermost layer of a future tracking detector at HL-LHC [1]. One challenge, when using diamond as a sensor material for such a detector, is to improve the charge collection efficiency. As trapping of charges is present even in unirradiated diamond, a figure of merit is the charge collection distance (CCD), i.e. the distance an electron-hole pair separates before the charge carriers are trapped. In order to collect the full charge from a sensor, the distance between the electrodes has to be smaller than the CCD. For planar electrodes, i.e. electrodes on the surface of the sensor, this distance equals its thickness. Using electrodes which penetrate the sample, the so-called 3D electrodes, decouples their spacing from the thickness. To produce these electrodes in a diamond sensor a phase change induced by a femtosecond laser is used [2]. The diamond lattice is thereby transformed into a combination of diamond-like carbon, amorphous carbon and graphite, which is conductive. Continuous channels are produced by moving the focal plane of the laser from the back to the front side [3].

Another advantage of the 3D electrode geometry is the lower bias voltage for the same electric field compared to planar electrodes. This also allows a faster charge collection. Due to these properties, 3D electrodes allow the use of less expensive low CCD diamonds, while still obtaining the full signal.

In this paper in Section 2 testbeam results with a 3D diamond sample are presented, and Section 3 shows Raman spectra and their interpretation of the conductive channels.

2.   Testbeam results

A single crystalline (scCVD) diamond sample of electronic grade with a thickness of 440 μm and a size of 4.7×4.7 mm^2 was used [4]. In this sample a total of 219 channels were grown using a Coherent Libra Ti-Sapphire femto-second laser with a wavelength of 800 nm. The laser was pulsed at 1 kHz with a pulse duration of 100 fs. The beam was focused to a spot size of about 4 μm with an energy density of 2 J cm^{-2}. The diamond sample was mounted on a 3-axis motorised stage and moved in the direction of the beam with a velocity of 20 μm s^{-1} with respect to the laser.

The diamond sample was metallised using the mask shown in Fig. 1. It is divided into three parts to allow testing of the influence of the metallisation and the conductive channels on the charge collection on the same sample. One part is a planar strip detector with a pitch of 50 μm, which allows comparison with traditional planar electrode sensors. The conductive channels of the 3D part are organised in cells with a size of 150×150 μm^2, each with a readout channel in the centre of the cell and four bias channels in the corners. These cells were connected column wise to a single readout. The metallisation pattern for this structure is duplicated once on the sample, but with no conductive channels underneath ("3D phantom"). This allows the measurement of the influence of the metallisation pattern on the charge collection.

The sample was read out by connecting each strip to a charge sensitive amplifier channel of a VA2 chip [5]. A

testbeam with 120 GeV pions was performed at the H6 CERN-SPS beam line. A silicon strip telescope, triggered by two external scintillators, provided particle tracking information [6]. The planar strip detector was biased with a voltage of 500 V (the diamond sensor showed full charge collection for bias voltages in excess of 450 V) and the two 3D structures with 25 V.

For each readout channel the initial pedestal and its width (σ) was determined using the first 500 events. The pedestal of later events was calculated using the 500 events directly prior to the event, while excluding signal events (i.e. events with more charge than 5σ). The pedestal and common mode were subtracted for each channel. Only events with one track were used in this analysis. The signal from the diamond was calculated by summing up the signal from the three channels closest to the predicted track position.

A negative signal response was observed for some channels at values which exceed the pedestal width by far. A cut was per- formed at -700 e which corresponds to $7:4\sigma$ of the pedestal width. The predicted track position of these events are predominantly located near bias electrodes. These channels have been identified as missing in resistance measurements. Missing readout electrodes can be identified by the significantly reduced signal measured in these cells.
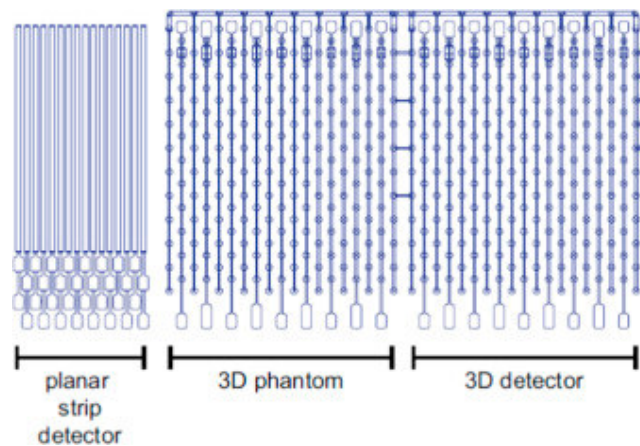

Fig. 1. Mask for the metallisation of the diamond sample [4]. It is divided into three parts. On the right a strip structure to connect all conductive channels ("3D detector"), which is repeated in the middle but without conductive channels underneath ("3D phantom") and on the left a planar strip detector.

For the analysis a fiducial region was defined on the 3D detector which contains no missing readout channels and few missing bias electrodes. Signals from the 3D detector show a most probable charge of 13,900 e compared to 4400 e for signals from the 3D phantom. This shows that the conductive channels do collect charges, as the influence of the metallisation is the same in both regions. The signal from the planar strip part has a most probable value of 13,800 e as shown in Fig. 2. It operates at a much higher bias voltage where full charge collection is expected for this diamond sample. This shows that with the 3D design it is possible to collect the full charge while applying a lower bias voltage.
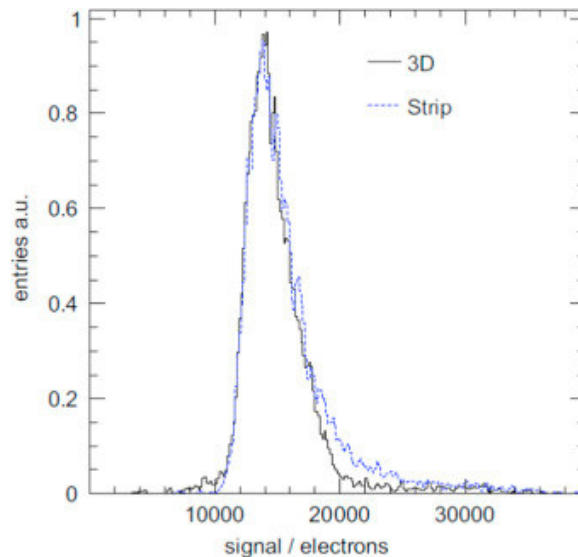
Fig. 2. Charge spectra from the 3D detector and from the strip detector [4]. The peak of the distribution is for the 3D detector at 13,900 e and for the strip detector at 13,800 e. The mean values are 15,000 e and 15,800 e for the 3D and for the strip detector, respectively.

3. Raman spectroscopy

A femtosecond laser is used to produce the conductive channels in diamond. The focal plane of this laser is moved from the back to the front of the sample. The reason for this is that the product of the phase change absorbs the laser radiation and thus prevents phase change of the diamond material downstream of the laser. This results in very different structures of the conductive channels on the surface of the diamond, where the laser focus enters ("seed side") or exits ("exit side") of the crystal.

On the seed side the conductive material is only irradiated by the first few pulses of the femtosecond laser as further pulses are absorbed by material grown upstream. This is not the case on the exit side, where the material is exposed for many pulses, which heat it up. This local heating results in a evaporation of parts of the grown channel, leading to a crater like structure. Such a crater can be disadvantageous for a good metal to conductive channel contact on this side. It could happen, that the crater is too narrow for the metal layer to reach the graphite at its bottom. A metallisation from both sides is needed for the application of the 3D diamond as a pixel detector.

Furthermore, in order to use it as a pixel detector, the resistivity of the conductive channels has to be uniform and low. The composition of the material after the phase change can depend on several parameters of the laser, like wavelength, pulse duration, and size of the focal plane. Most of these are fixed for a given setup, so usually the only variable parameters for an optimisation of the growth are the fluence of the beam and the velocity of the focal plane through the diamond. For production of a larger amount of 3D diamond sensors, which could be e.g. for a tracking detector, a low production time is crucial. To achieve this, generally more than one available femtosecond laser is advantageous, but also femtosecond lasers which are pulsed at a higher frequency. The difference of the growth of conductive channels in single crystalline and lower grade poly crystalline (pCVD) diamond should also be studied.

For these reasons, a total of 246 conductive channels were grown in a pCVD diamond sample of 500 μm thickness. These channels were produced at Laser-Laboratorium Göttingen e.V. using a Yb:YAG femtosecond laser with a wavelength of 1043 nm. The pulse duration was 290 fs with a repetition rate of 200 kHz. The diameter of the focal plane was about 1.6 μm. In order to determine the best growth parameters with this setup, four power settings and four velocities of the diamond with respect to the laser were tested. These values covered a large parameter space, namely 10, 25, 60, 150 mW for the power and 50, 200, 2000, 10,000 μm s^{-1} for the velocity. For each combination of these two parameters, at least five channels were produced. The success rate for a conductive channel without any interruptions was determined by optical inspection to be 88%.

In order to measure the influence of these parameters on the phase change, especially on the exit side, Raman spectroscopy was performed. The measurement of the Raman spectra was performed using a laser with a wavelength of 440 nm and a spot size of about 2 μm. This is significantly smaller than the diameter of the smallest conductive channel, which is about 4 μm. Prior to the measurement of the conductive channels two reference measurements were performed. The first measurement, with the laser focused in a region where no conductive channels are present in the diamond sample, yielded a narrow peak at 1332 nm^{-1} as expected for pure diamond. In the second measurement a highly conductive graphite sample was used. It showed two broad peaks of nearly the same amplitude at approximately 1580 nm^{-1} and 1350 nm^{-1}. These peaks are called the g- and d-peak, respectively. The first one is attributed to ordered graphite, the second one to unordered graphite [7].

In all spectra of the conductive channels a clear contribution from graphite, indicated by the g- and d-peak, is visible, although it varies in intensity. For almost all spectra, except for a few with high energy and high velocity, a diamond peak is noticeable. This peak strongly varies in intensity, being suppressed for high energy and high velocity while being dominant for low energy or low velocity. In general, the diamond contribution is more apparent on the exit side. This is expected, as part of the material is evaporated, leaving behind a crater-like structure.

To evaluate the spectra, they are fitted by a combination of five Gaussian distributions and a linear function describing the peaks and the background, as shown in Fig. 4. Since the diamond peak is very narrow and consists of roughly five data points, the fit quality on this peak in the combined fit is generally poor. Thus for the extraction of the diamond peak value, an extra Gaussian fit in the region between 1327 nm^{-1} and 1340 nm^{-1} is performed.

As a rough figure of merit for the quality of the channels, the ratio of the height of the diamond peak to the height of the g-peak is calculated. The result is shown in Fig. 3. For low energies of 10 mW and low velocities of 50 μm s^{-1} the ratios from the individual channels on the seed side are highly fluctuating. This indicates, that the energy needed for the phase transition is barely reached and only little conductive material is created. For the seed side higher energies and velocities yield all reasonable low ratios. On the exit side only channels grown with a velocity of 2000 μm s^{-1} or faster have enough remaining graphite in the crater like structure to be measured with Raman spectroscopy. Here for energies above 60 mW the diamond contribution is fairly low.
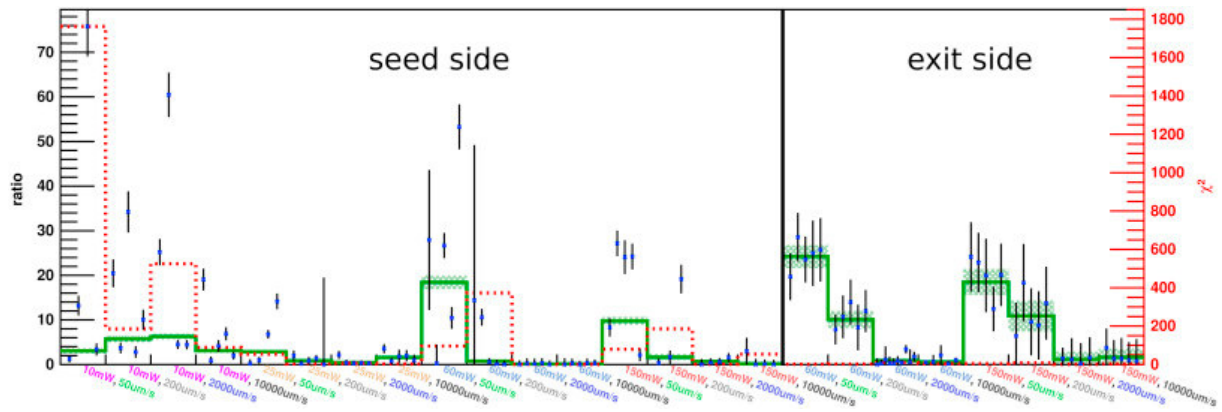
Fig. 3. Ratio of the value of the diamond peak to the value of the g-peak. Results for individual channels are marked by a blue cross, the weighted mean for each setting is indicated by the green line. The red dotted line shows the χ^2 value for each setting. (For interpretation of the references to color in this figure caption, the reader is referred to the web version of this paper.)
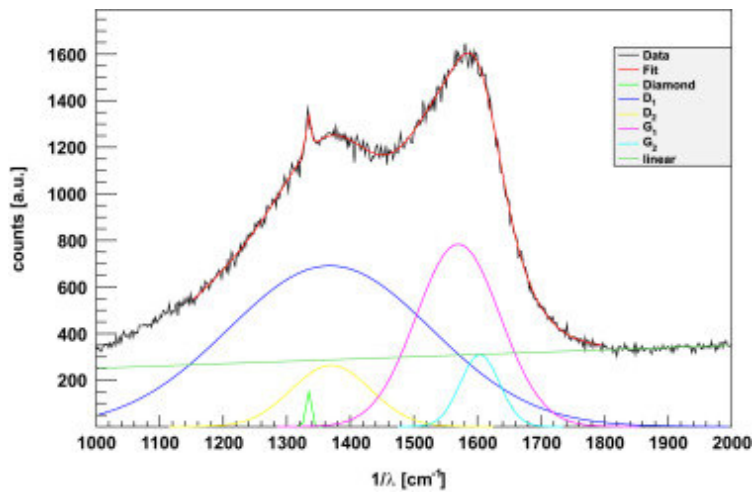

Fig. 4. Raman spectrum for the seed side of a channel grown at 60 mW and 2000 μm s^{-1}. Individual contributions of the fitted functions are shown.

4.   Conclusion

Results from a testbeam of a scCVD diamond with 3D electrodes show, that these channels do collect charges. This technique allows the full collection of the deposited charge even for samples with a CCD lower than their thickness. The best settings for a femtosecond laser setup have been investigated with a pCVD diamond. Results show a systematic difference of the structure of the conductive channels on the seed and exit side.

Acknowledgements

References

[1]   C. Bauer, et al., Nuclear Instruments and Methods in Physics Research in Section A 367 (1995) 207.

[2]   T.V. Kononenko, et al., Applied Physics A90 (2008) 645.

[3]   T.V. Kononenko, et al., Diamond and Related Materials 20 (2011) 264.

[4]   F. Bachmair, et al., Nuclear Instruments and Methods in Physics Research in Section A 786 (2015) 97.

[5]   Integrated Detectors& Electronics AS, Data Sheet VA2 Readout Chip, Oslo, Norway, 2014.

[6]   C. Colledani, et al., Nuclear Instruments and Methods in Physics Research in Section A 372 (1996) 379.

[7]   A.C. Ferrari, J. Robertson, Physical Review B 61 (2000) 14095.